Program Record (EERE Offices of Fuel Cell, Vehicle, and Bioenergy Technologies)		
Record #: 17005	**Date:** June 23, 2017	
Title: Water Consumption for Light-Duty Vehicles' Transportation Fuels		
Originators: Jeongwoo Han and Amgad Elgowainy (Argonne National Laboratory)		
Peer reviewed by: Dr. George Parks, Diana Bauer		
Approved by: Fred Joseck (DOE-FCTO), Rachael Nealer (DOE-VTO), Zia Haq (DOE-BETO)	**Date:** June 23, 2017	

Items

This record provides the life-cycle analysis results on freshwater consumption associated with various transportation fuels for use in light-duty vehicles (LDVs) in the United States. The life-cycle water consumption for fuel cell electric vehicles (FCEVs) can be comparable to that for conventional gasoline vehicles for certain fuel pathways. The values range from roughly 9 to 65 gallons of water per 100 miles driven depending on the pathway for hydrogen production, delivery, storage and dispensing. The baseline life-cycle water consumption for conventional gasoline vehicles (with 10% ethanol) is roughly 23 gallons per 100 miles driven. Detailed sensitivity analysis is documented below and assumptions will be updated periodically as technologies advance.

Data, Assumptions, References

This record estimates life-cycle water consumption for a range of vehicle-fuel technology pathway options. Two terms commonly refer to water use in a given process: water withdrawal and water consumption. Water withdrawal represents the amount of water uptake from a surface or ground water source. On the other hand, water consumption refers to the amount of water that becomes unavailable for other uses in the same water resource region. For example, water discharged from fuel production plants may not be considered consumed since it is usually treated and becomes available for future use in the same region. Generally, there are three major causes of water consumption: evaporation, incorporation into products, or degradation to a quality not appropriate for future use (Lampert et al. 2014).

Table 1. Transportation Fuel/Vehicle Pathways Analyzed

Pathway	Description
Gasoline Blendstock- ICEV (for benchmarking with gge results)	Internal combustion engine vehicle (ICEV) on gasoline (almost all U.S. gasoline is E10 as of 2013, so this serves as a benchmark to see how various gasoline/ethanol mixtures differ from pure gasoline)
Diesel ICEV	ICEV using diesel from petroleum
Gasoline E10 ICEV (for benchmarking with per-100-miles-driven results)	ICEV using a mixture of 90% petroleum gasoline blendstock and 10% corn ethanol (by volume)
E85 ICEV (corn)	ICEV using gasoline-ethanol blends containing 85% denatured ethanol (by volume) from corn grains
CNG ICEV	ICEV using compressed natural gas (CNG)
BEV (grid electricity)	Battery electric vehicle (BEV-210) using average U.S. grid electricity generation

	mix (300-mile nominal range, 210-mile realistic, on-road range)
BEV (solar)	BEV-210 using solar electricity, a mix of photovoltaic (PV) and concentrated solar power (CSP)
FC Distributed NG SMR	Fuel cell hybrid electric vehicle (FCEV) using H_2 produced from natural gas (NG) via steam methane reforming (SMR) at a retail fueling station
FC Distributed Electrolysis (U.S. grid mix)	FCEV on H_2 produced via electrolysis of water using average U.S. grid electricity generation mix at a retail fueling station
FC Distributed Electrolysis (solar)	FCEV on H_2 produced via electrolysis using solar power at a retail station
FC Central NG SMR w/ Pipeline Transport	H_2 produced at a central SMR location and pipelined to retailing stations
FC Central NG SMR w/ CCS and Pipeline Transport	As above, but with carbon capture and storage (CCS)
FC Central Wind w/ Pipeline Transport	FCEV on H_2 produced via electrolysis using wind power at a central location (pipelined to retail stations)
FC Central Biomass w/ Pipeline Transport	FCEV using H_2 produced via hybrid poplar gasification at a central location (pipelined to retail stations)
FC Central Biomass w/Liquid H_2 Truck Transport	FCEV using H_2 produced via hybrid poplar gasification at a central location, with subsequent liquefaction of H_2 for truck delivery to retail stations
FC Central Coal w/ CCS and Pipeline Transport	FCEV using H_2 produced via coal gasification with CCS at a central station (pipelined to retail stations)

While water is one of the most abundant resources on the earth, available water generally refers to freshwater only because freshwater is a limited resource with large demand for various purposes. This record considers only the consumption of freshwater along fuel-production pathways; thus, it excludes non-freshwater consumption (e.g., saline, brackish, and treated wastewater).

Table 1 describes the transportation vehicle-fuel pathways considered in this record. To compare water consumption associated with different fuel production pathways comprehensively, a comprehensive accounting of water consumption along the life cycle of the fuel needs to be conducted. A life-cycle analysis of transportation fuels is often called a well-to-wheels (WTW) analysis, covering key life-cycle stages from well (e.g., feedstock recovery) to wheels (e.g., vehicle operations). This record employed the Greenhouse gases, Regulated Emissions and Energy use in Transportation (GREET) model, developed by Argonne Laboratory, to conduct WTW water consumption analyses.

Figure 1 presents the system boundaries and key life-cycle stages of the vehicle-fuel pathways investigated in this record. The ICEV, BEV, and FCEV pathways are colored with gray, purple, and green, respectively. The gasoline, diesel, and ethanol pathways consist of five stages:

- feedstock recovery (i.e., crude recovery and corn farming) and transport,
- fuel production (i.e., gasoline and diesel from crude refining, and ethanol production),
- fuel transportation and distribution (T&D), and
- fuel consumption during vehicle operation.

Note that the E10 and E85 pathways include a process of blending gasoline blendstock for oxygenated blending (BOB) and ethanol. The CNG pathway starts with NG recovery and transport, followed by NG processing, transmission, and distribution. Lastly, NG is compressed at retail stations to fuel CNG vehicles. Alternatively, NG from a processing plant can be transported and distributed to refueling stations, where it is converted onsite to H_2 via SMR and compressed to be fuel for FCEVs. In large markets of hydrogen FCEVs, NG may be transported to central SMR plants (with or without CCS), where it is converted to H_2. Hydrogen can then be transported and distributed by pipelines to H_2 refueling stations. Note that for simplicity, the electricity pathway in Figure 1 represents the feedstock production and transport to power plants in an aggregated stage. However, separate calculations were conducted for each feedstock pathway (e.g., NG, coal, nuclear, residual oil, biomass, and other renewables), and the results were aggregated by the generation mix defined in Section 3.8. Electricity generated from these feedstocks is then transported and distributed to BEV charging stations. Alternatively, electricity can be used for H_2 production via distributed electrolysis (i.e., at refueling retail sites) for use in FCEVs. Moreover, instead of grid electricity, solar power can be used for recharging BEVs and H_2 production for FCEVs. For central production of hydrogen via electrolysis, wind power is assumed to be the source of electricity. The H_2 is transported and distributed from the central production site to refueling stations, where it is compressed for dispensing into FCEVs. For biomass and coal gasification pathways, the biomass or coal feedstock is farmed or mined, transported, and gasified at a central plant to produce H_2, which is subsequently transported and distributed for compression at refueling stations into FCEVs. Note that this record includes a liquid H_2 delivery pathway in which hydrogen is produced in a central biomass gasification plant, liquefied, and transported to fueling stations via cryogenic tankers. In such a case, no compression is needed at the refueling site since a liquid pump can increase the hydrogen pressure with a modest energy consumption, followed by a temperature increase in a heat exchanger before dispensing into FCEVs. Liquefaction takes significantly more electricity than compression for packaging purposes, but results in higher volumetric energy density and lower transportation cost compared to transporting compressed gaseous hydrogen. The impact of the electricity use for liquefaction and compression for each of these two options is included in the life-cycle water consumption results presented in the following section.

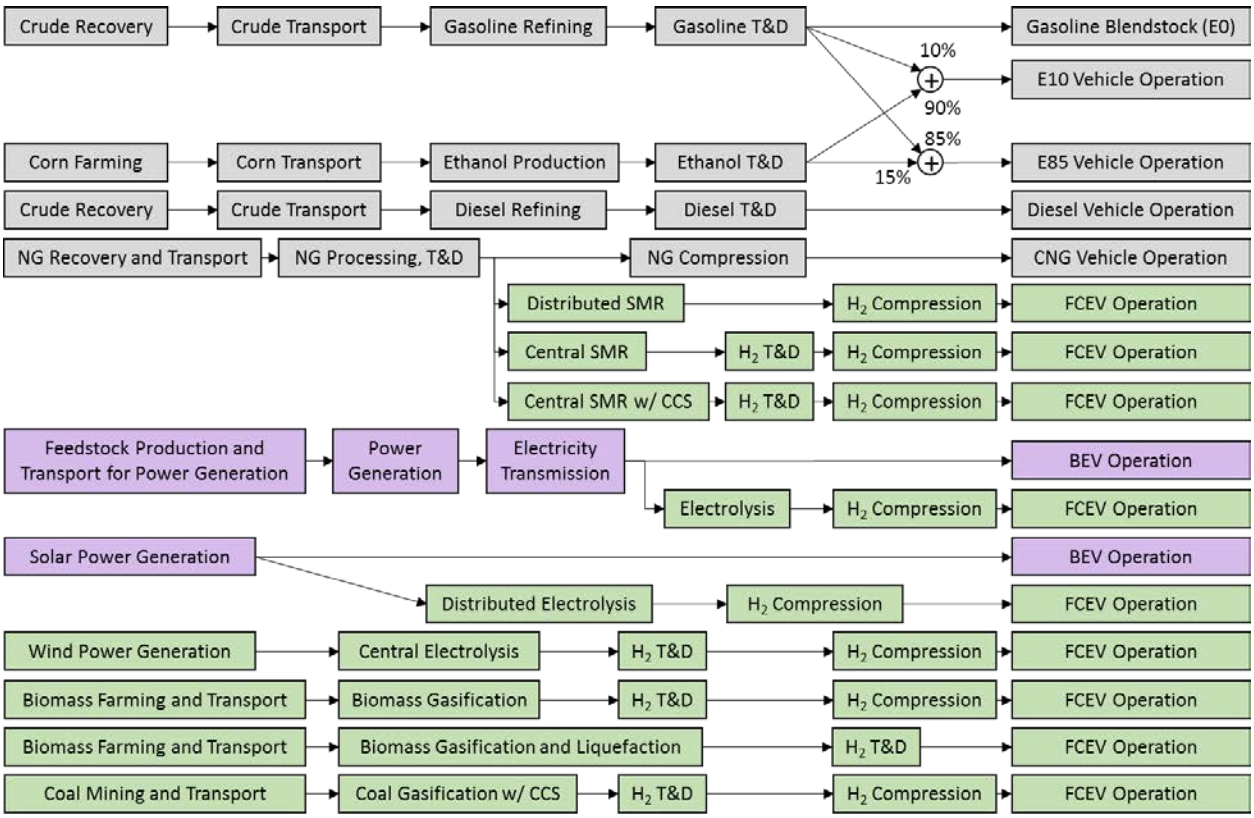

Figure 1. System boundaries of fuel and vehicle pathways

Life-cycle water consumption results are presented in Section 1 in gallons for two functional units: an energy unit of gasoline gallon equivalent (gge) and a service unit of 100 miles driven. An energy functional unit (e.g., gge) is useful in comparing different energy products in the same technology application. On the other hand, a service functional unit (e.g., 100 miles driven) can compare different vehicle-fuel pathways that provide the same service. Note that the vehicle fuel economy is the key factor converting gge results into 100-miles-driven results, and this adds additional uncertainty to the life-cycle water consumption results when provided in a service functional unit.

To investigate the impact of uncertainties and variabilities in parametric assumptions for life-cycle water consumption, we employed Monte-Carlo simulations with 1000 samples that used the stochastic simulation feature in the GREET model. Distributions functions for 30 major water consumption factors (WCFs) were developed and incorporated in the GREET model, as summarized in Section 5.

1. Results

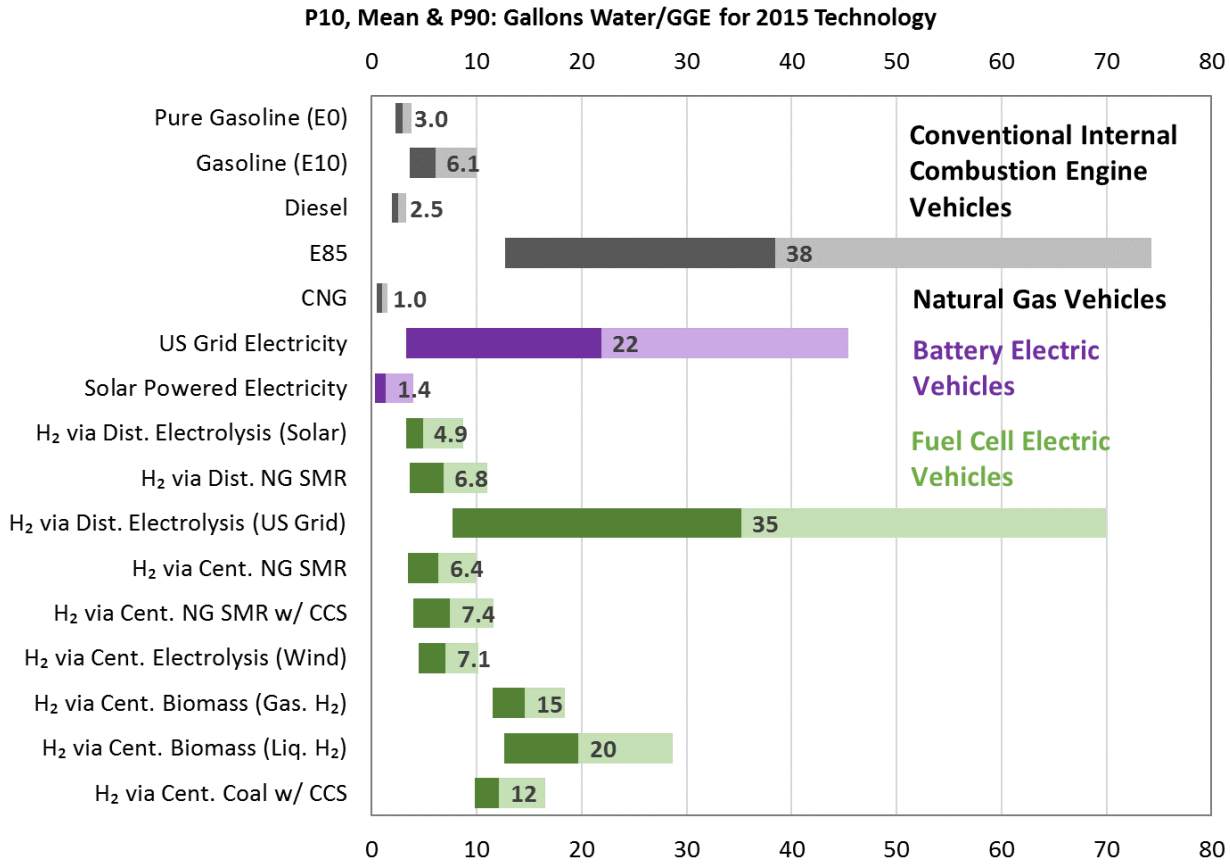

Figure 2. Life-cycle water consumed per gasoline gallon equivalent (gge) of fuel

Figure 2 presents the estimated amount of life-cycle water associated with the production and delivery of a gge of fuel. The lower and upper ends of each bar represent the 10th percentile (P10) and 90th percentile (P90) of the distributions determined from Monte-Carlo simulations, while the boundaries between the dark and bright portions of the bar (as well as the numeric values) denote the mean values from the distribution. On average, the most water-intensive fuel is E85 due to a large amount of water consumption in corn irrigation, followed by H_2 via electrolysis using the U.S. grid electricity mix, while the U.S. grid electricity itself ranks third. The U.S. grid electricity shows high water consumption intensity, largely due to the evaporative water loss from reservoirs for hydropower dams (although the hydropower generation share in the U.S. mix is only 6%). Detailed discussion on hydropower water consumption is provided in Section 3.8.2 (see Lee, et al. 2017 for more details). The high water intensity of U.S. grid electricity has a major impact on H_2 pathways because hydrogen compression or liquefaction processes consume large amounts of electricity on a per energy functional unit basis (i.e., gal/gge). The life-cycle water consumption of H_2 pathways via NG SMR, distributed electrolysis using solar power, and central electrolysis using wind power is comparable to that of baseline gasoline E10, while hydrogen production via biomass and coal gasification shows greater water consumption compared to that of gasoline E10. Note that the uncertainty (i.e., P10 to P90) ranges of E85 and the paths relying on average U.S. electricity grid (BEV 210 and electrolysis FCEV) have more uncertainty than the others due to the

large variations in irrigation for corn and evaporation from hydropower reservoirs, respectively. More details on water consumption by these pathways are provided in Section 3.

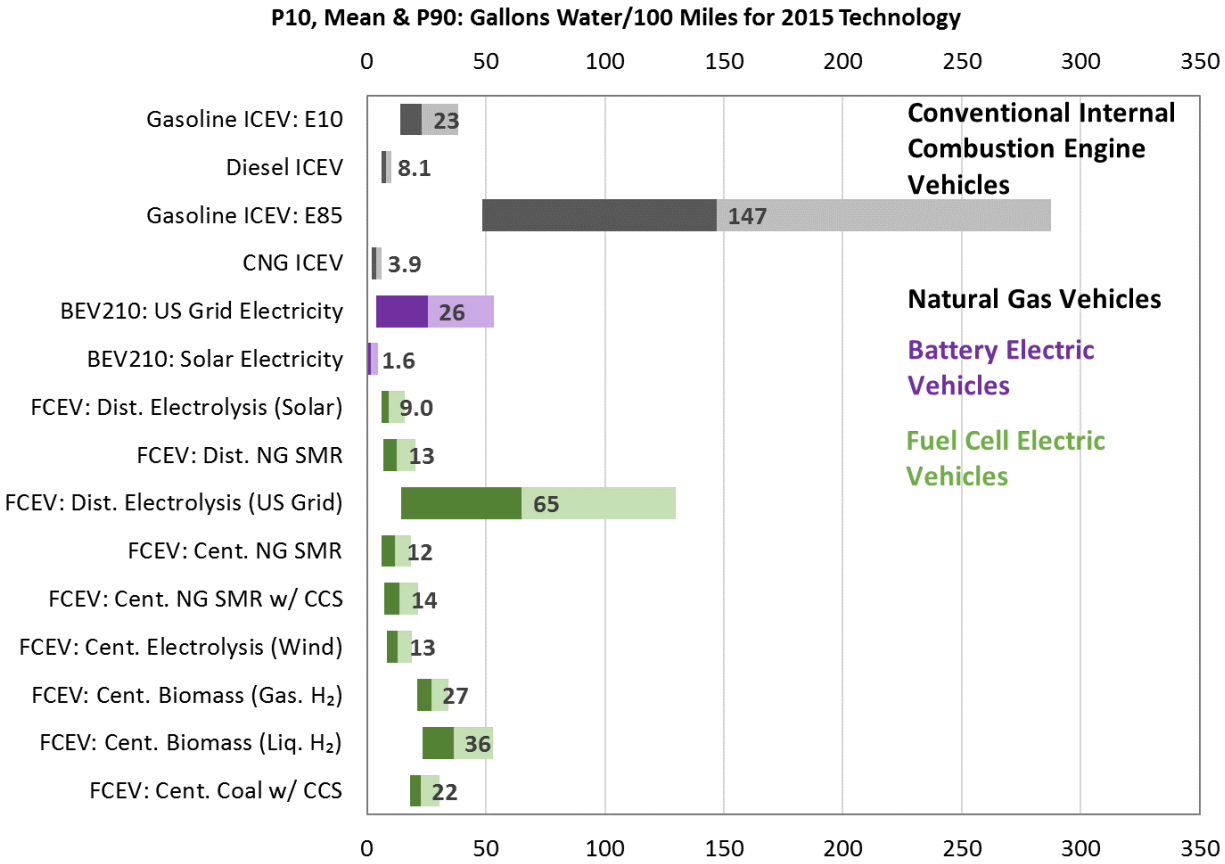

Figure 3. Life-cycle water consumption per 100 miles driven

Figure 3 provides the life-cycle water consumption in gal/100 miles driven by incorporating vehicle fuel economy. With this service functional unit, water consumption associated with corn E85 vehicles shows the highest life-cycle water consumption at 147 gal/100 miles compared to all other vehicle-fuel pathways. FCEVs powered by H_2 via electrolysis using the U.S. electricity grid mix also show a high life-cycle water consumption of 65 gal/100 miles. Other FCEV and BEV pathways such as BEVs with U.S. grid electricity and FCEVs with biomass or coal gasification have life-cycle water consumption comparable to baseline gasoline E10 ICEV. BEVs with solar electricity, FCEVs with NG SMR, distributed electrolysis using solar power, and central electrolysis using wind power have lower life-cycle water consumption compared to that of gasoline E10 ICEVs. BEVs with solar power have the lowest life-cycle water consumption followed by CNG ICEVs, while FCEVs with H_2 from solar power have life-cycle water consumption similar to that of diesel ICEVs.

Table 2. Water Consumption Results for Each Stage (gal/100 miles). (The values in the parentheses denote the P10 and P90 uncertainty values.)

	Crude/ NG/Coal Recovery & Transport	Gasoline/ Diesel/NG Production	Corn/ Biomass Farming & Transport	Feedstock Production and Transport for Power Generation	Power Generation	Ethanol/H_2 Production	Fuel T&D	NG/H_2 Compression and H_2 Liquefaction	WTW
Gasoline ICEV (E10)	6.2 (4.7 - 8.2)	4.3 (3.3 - 5.4)	11 (2.7 - 22)			1.5 (1.3 - 1.7)	0.0 (0.0 - 0.0)		23 (14 - 38)
Gasoline ICEV (E85)	1.6 (1.2 - 2.0)	1.1 (0.8 - 1.3)	127 (31 - 257)			17 (15 - 20)	0.0 (0.0 - 0.0)		147 (48 - 288)
Diesel ICEV	6.4 (4.8 - 8.4)	1.6 (1.1 - 2.0)					0.1 (0.0 - 0.1)		8.1 (6.0 - 10.2)
CNG ICEV	1.0 (0.6 - 1.6)	0.9 (0.8 - 1.0)					0.1 (0.1 - 0.2)	1.9 (0.3 - 4.0)	3.9 (2.0 - 6.1)
BEV: Grid				1.3 (1.0 - 3.3)	24.3 (2.2 - 52.2)				26 (3.8 - 54)
BEV: Solar					1.6 (0.3 - 4.7)				1.6 (0.3 - 4.7)
FCEV Distributed Solar					3.5 (0.8 - 10.2)	5.3 (5.1 - 5.5)		0.3 (0.1 - 0.8)	9.0 (6.1 - 16)
FCEV Distributed NG SMR	0.6 (0.3 - 0.9)	0.5 (0.5 - 0.6)				7.3 (5.0 - 10.7)	0.1 (0.0 - 0.1)	4.1 (0.6 - 8.7)	13 (6.7 - 20)
FCEV Distributed U.S. Grid				2.8 (2.3 - 7.1)	53 (4.7 - 114)	5.3 (5.1 - 5.5)		4.1 (0.6 - 8.5)	65 (14 - 130)
FCEV Central NG SMR	0.6 (0.3 - 1.0)	0.6 (0.5 - 0.6)				5.1 (4.4 - 5.9)	1.3 (0.2 - 2.8)	4.1 (0.6 - 8.5)	12 (6.3 - 18)
FCEV Central NG SMR w/ CCS	0.6 (0.3 - 1.0)	0.6 (0.5 - 0.6)				7.1 (5.5 - 9.1)	1.3 (0.2 - 2.8)	4.1 (0.6 - 8.5)	14 (7.4 - 22)
FCEV Central Wind					0.1 (0.0 - 0.1)	7.5 (7.2 - 7.7)	1.3 (0.2 - 2.8)	4.1 (0.6 - 8.5)	13 (8.3 - 19)
FCEV Central Biomass			14 (14 - 15)			7.5 (6.4 - 8.7)	1.3 (0.2 - 2.8)	4.1 (0.6 - 8.5)	27 (21 - 34)
FCEV Central Biomass, Liq. H_2			14.5 (14.0 - 15)			7.7 (6.6 - 9.0)	0.0 (0.0 - 0.0)	14.1 (2.1 - 30)	36 (23 - 53)
FCEV Central Coal CCS	1.8 (1.5 - 6.3)					15.2 (14.6 - 15.6)	1.3 (0.2 - 2.8)	4.1 (0.6 - 8.5)	23 (18 - 31)

Table 2 provides water-consumption numerical results for each step of the fuel life cycle. As discussed above, the most water intensive stages include corn farming (i.e., irrigation), U.S. grid electricity generation (evaporation from hydropower reservoirs), and H_2 liquefaction and compression (consuming a substantial amount of U.S. grid electricity).

2. Conclusions

Average life-cycle water consumption associated with the majority of BEV and FCEV pathways (other than H_2 production via water electrolysis using U.S. grid electricity) ranges from 9 to 36 gal/100 miles driven as compared to 23 gal/100 miles driven by gasoline E10 ICEVs with corn ethanol. On average, BEV-210s consume the smallest amount of water at 2 gal/100 miles when solar power is used, while the water consumption increases to 26 gal/100 miles when U.S. grid electricity is used. Similarly, on average, FCEVs with H_2 from electrolysis using U.S. grid electricity consumes a large amount of water (65 gal/100 miles), but are much less water intensive compared to E85 ICEVs with corn ethanol (147 gal/100 miles). Diesel and CNG ICEVs consume a smaller amount of water (8 and 4 gal/100 miles, respectively).

Major water consumption processes include irrigation for corn farming, evaporative loss from hydropower reservoirs, and indirect (upstream) losses associated with H_2 liquefaction and compression using a U.S. grid electricity mix. The large water consumption for corn ethanol pathway can be reduced if a less water-intensive cellulosic biomass is used as the feedstock. While evaporative loss from hydropower reservoirs is inevitable (largely determined by climate and other design conditions), these hydropower dams are located in freshwater-rich regions. Therefore, the regional impacts of hydropower on water availability warrant further investigation.

3. Assumptions and Supporting Data

The water consumption results in this record were generated by using the GREET 2016 model (October in 2016). The target year is set to 2015. This record developed the distribution functions of the WCFs presented in Table 3, which were incorporated in GREET for stochastic simulation.

Development of the WCFs was based on the following considerations:

1. When a large number of samples of WCFs are available, such as those for corn irrigation and thermo- and hydro-power generation, a distribution function is developed by fitting the actual water consumption factors (weighted by production volumes) to one of the eleven distribution functions built in the GREET model.
2. When the available WCF data are not sufficient to develop a distribution function,
    a. a triangular distribution function is first attempted so that the minimum, maximum, and average of the samples match the minimum, maximum, and mean of the triangular distribution, or
    b. if the samples are too skewed for a triangular distribution function to be developed, a Weibull distribution function is used where the minimum, maximum, and average of the samples match the zeroth percentile (P0), 90th percentile (P90), and mean of the triangular distribution, respectively.

Details of key parameters and adjustments for this record are presented in this section.

Table 3. Distribution Function of Water Consumption Factors in this Record

Distribution by fitting actual water consumption factors weighted by production volumes				
Parameter	Type	Mean	P10	P90
Bakken shale oil extraction (gal/mmBtu)	Lognormal	1.44	0.50	3.56
Eagle Ford shale oil extraction (gal/mmBtu)	Gamma	2.20	0.68	4.35
Corn farming irrigation (gal/bushel)	Lognormal	146	6.6	322
Steam turbine power generation (gal/kWh)	Lognormal	0.40	0.06	0.88
Combined cycle power generation (gal/kWh)	Lognormal	0.16	0.01	0.36
Hydropower generation with reservoir (gal/kWh)	Lognormal	5.65	0.08	10.5
Triangular distribution used due to lack of data				
Parameter	Type	Mean	Min	Max
On-shore conventional crude oil extraction (gal/mmBtu)	Triangular	26.5	16.2	41.6
Gasoline refining (gal/mmBtu)	Triangular	5.47	3.96	8.18
Diesel refining (gal/mmBtu)	Triangular	2.56	1.47	4.17
Jet refining (gal/mmBtu)	Triangular	1.19	0.98	1.54
Liquefied petroleum gas refining (gal/mmBtu)	Triangular	4.36	3.25	6.48
Residual fuel oil refining (gal/mmBtu)	Triangular	1.63	1.21	2.22
Naphtha refining (gal/mmBtu)	Triangular	1.25	1.03	1.63
Petroleum coke refining (gal/mmBtu)	Triangular	1.85	1.56	2.41
Conventional gas extraction (gal/mmBtu)	Triangular	0.11	0.07	0.16
Shale gas extraction (gal/mmBtu)	Triangular	3.66	1.75	5.56
Coal underground mining (gal/mmBtu)	Triangular	4.64	1.90	6.70
Uranium enrichment (gal/g U-235)	Triangular	81.4	69.1	100
Uranium conversion, fab. and waste storage (gal/g U-235)	Triangular	97.0	41.6	145
Wind power generation (gal/kWh)	Triangular	0.001	0.000	0.002
Enhanced geothermal system (gal/ kWh)	Triangular	0.510	0.290	0.720
Hydrogen via NG central SMR w/o CCS (gal/mmBtu)	Triangular	21.1	19.3	22.0
Hydrogen via NG central SMR w/ CCS (gal/mmBtu)	Triangular	25.5	23.7	26.4
Hydrogen via coal gasification (gal/mmBtu)	Triangular	73.1	72.5	73.7
Hydrogen via biomass gasification (gal/mmBtu)	Triangular	30.3	28.8	32.4
Weibull distribution used due to lack and substantial skewness of data				
Parameter	Type	Mean	P0	P90
Canadian oil sands in-situ recovery (gal/mmBtu)	Weibull	5.47	1.97	26.3
Coal surface mining (gal/mmBtu)	Weibull	2.60	1.70	16.1
Uranium extraction (gal/g U-235)	Weibull	201	37.7	798
Solar power generation (gal/kWh)	Weibull	0.04	0.01	0.11
Flash geothermal (gal/ kWh)	Weibull	1.20	0.69	3.80
Binary geothermal (gal/ kWh)	Weibull	1.70	1.51	4.60
Hydrogen via NG distributed SMR (gal/mmBtu)	Weibull	22.0	21.1	26.4

3.1. Midsize Cars' Fuel Economy

Table 4 summarizes the midsize cars' fuel economy of Model Year 2015 used in this record, which were estimated with Argonne National Laboratory's Autonomie model (Elgowainy et al. 2016b). In the following, MPGGE denotes miles per gasoline gallon equivalent. Note that battery electric vehicles with 210 miles "on-road" driving range (BEV-210) are considered in this record. The ratios of fuel economy of ICEVs (E85, diesel, and CNG), BEVs, and FCEVs relative to that of conventional gasoline (E10) vehicles are set to 1, 1.2, 0.95, 3.24, and 2.07, respectively.

Table 4. On-Road (Adjusted) Vehicle Fuel Economy and Ratio of Fuel Economy to Regular Gasoline Vehicles' Fuel Economy for Midsize Cars of Model Year 2015

Vehicle Technology	Fuel Economy (MPGGE)	Fuel Economy Ratio
Gasoline (E10) Vehicle	26.2	
Gasoline (E85) Vehicle	26.2	1.00
Diesel Vehicle	31.6	1.21
CNG Vehicle	24.9	0.95
Battery Electric Vehicle (BEV-210)	84.7	3.24
Fuel Cell Electric Vehicle	54.1	2.07

The distribution function of gasoline (E10) vehicles was developed in Brinkman et al. (2005) as a Weibull distribution with P10, mean, and P90 of 23.9, 28, and 33, respectively. Since the updated fuel economy of gasoline (E10) vehicles in this record is lower than the mean fuel economy of the distribution, the fuel economy distribution is scaled down to match the scaled-down mean to the updated fuel economy of 26.2, resulting in P10 and P90 of 22.4 and 30.9, respectively. The distribution functions of fuel economy for other vehicles are calculated by multiplying the fuel economy ratios in Table 4 and the gasoline (E10) vehicles' distribution function.

3.2. Crude Oil Extraction and Refining

The WCFs of crude oil extraction vary by crude oil type: conventional crude oil, shale oil, and Canadian oil sand. The shares of the crude oil sources are presented in Table 5 (Lee et al. 2016a). Off-shore conventional crude recovery is assumed to consume no fresh water, considering the large availability of sea water. Foreign conventional crude oil recovery is assumed to be on-shore and to have the same water consumption factors as U.S. domestic conventional crude oil recovery (on-shore) because of lack of information on foreign conventional crude recovery.

Table 5. Share of Crude Sources in 2015 (Lee et al. 2016a)

	U.S. (Domestic)			Canadian Oil Sand	Foreign Conventional Crude
	Conventional Crude		Shale Oil		
	On-Shore	Off-Shore			
Share	28.3%	10.0%	17.9%	10.3%	33.5%

Wu and Chiu (2011) estimated the WCFs of on-shore conventional crude oil extraction by the Petroleum Administration for Defense District (PADD): PADDs II, III, and V have WCFs of 2.1, 2.3, and 5.4 gal/gal of crude oil, respectively, while PADDs I and IV consume a negligible amount of water. Based on Wu and Chiu (2011) and the 2005 on-shore oil production volumes reported by the U.S. Energy Information Administration (EIA 2008), Lampert et al. (2014) derived a production-weighted WCF of 26.5 gal water per mmBtu of crude (lower heating value based). Since the oil production in PADDs I and IV is much smaller than that of the other PADDs, this record used the WCFs of PADDs II and V as the minimum and maximum WCF for on-shore conventional crude oil extraction, respectively (16.2 and 41.6 gal/mmBtu).

A large share of U.S. shale oil comes from Bakken and Eagle Ford, accounting for 26% and 33% of U.S. shale oil production in 2015, respectively (U.S. EIA 2016c). Using monthly operating data from 2006 to 2013 provided by the North Dakota Department of Mineral Resources, Brandt et al. (2015) conducted extensive investigation on shale oil extraction in Bakken. Based on the monthly operating data, the production-weighted WCF of Bakken shale oil extraction was estimated as 1.44 gal/mmBtu and has a lognormal distribution whose P10 and P90 are 0.50 and 3.56 gal/mmBtu, respectively. Similarly, using monthly operating data from 2009 to 2014 provided by IHS-Bureau of Economic Geology, Ghandi et al. (2015) investigated shale oil extraction in Eagle Ford and estimated its WCF to be 2.20 gal/mmBtu with a gamma distribution (0.68 and 4.35 gal/mmBtu for P10 and P90, respectively).

Canadian oil sands can be recovered by surface mining and in-situ production, which have significantly different WCFs. Wu and Chiu (2011) estimated the surface-mining WCF at 4.0 gal/gal oil sands and presented three WCFs for in-situ production by recovery technology: 0.3 for steam-assisted gravity drainage, 1.2 for cyclic steam stimulation, and 4.0 for multi-scheme. They estimated that upgrading of bitumen to synthetic crude oil (SCO) would consume 1 gal water per gal SCO. Based on Wu and Chiu (2011), Lampert et al. (2014) derived WCFs of 27.45 gal/mmBtu for surface mining recovery, 5.5 gal/mmBtu for in-situ recovery, and 6.9 for bitumen upgrading to SCO. The distribution of in-situ recovery is defined as a Weibull distribution by using the range defined in Wu and Chiu (2011): P0 at 1.97 gal/mmBtu and P90 at 26.3 gal/mmBtu.

Petroleum refineries convert crude oil into various petroleum products, such as gasoline, diesel, jet, liquefied petroleum gas (LPG), residual fuel oil (RFO), naphtha, and petroleum coke. Petroleum refineries consist of various process units, which require cooling and/or process water. The cooling water demands by each process unit could vary significantly depending on the size of the process unit, the cost and availability of water, and the relative cost of electricity versus capital. Moreover, the configuration of refineries varies widely. To address the variation in cooling technology and refinery configuration, Henderson (2016) estimated the water consumption for three refinery configurations using three levels of cooling demands. The three refinery configurations include cracking (refineries with a fluid catalytic cracker [FCC]), light coking (refineries with FCC and coker), and heavy coking (refineries with FCC, coker, and hydrocracker). Cracking, light coking, and heavy coking refineries account for 17%, 63%, and 20% of total U.S. refinery capacity, respectively. The three cooling water demands include typical cooling water usage, 20% lower usage than typical, and 50% higher usage than typical. The water

consumption by each process unit was allocated to final product pools depending on the contributions of the process unit to components in the final products. With the typical cooling water usage, the capacity-weighted WCFs of petroleum products are presented in Table 3. The triangular distribution is used for these WCFs. The minimum and maximum from the nine cases examined in Henderson (2016) (3 configurations x 3 cooling water demands) are used as the minimum and maximum of the triangular distributions, respectively.

3.3. Corn Farming and Ethanol Production

A corn ethanol production pathway includes corn farming and transport, ethanol production, transportation and distribution, and end use of ethanol blended with gasoline in vehicles. In this production pathway, irrigation for corn farming is a major water consumer. Wu and Chiu (2011) collected state-level irrigation acreage and depths from the 1998, 2003, and 2008 surveys to estimate state-level water withdrawal for corn farming irrigation. Using the state-level withdrawal and the state-level ratio of water consumption and withdrawal for corn farming irrigation in 1995 as provided by Solley et al. (1998), Lampert et al. (2014) estimated state-level water consumption in 2008. Moreover, they calculated the state-level WCFs using 2007 corn production from the U.S. Department of Agriculture (USDA 2009) as shown in Table 6. Based on these WCFs and corn production volumes in different states, this record developed a lognormal distribution for corn farming irrigation (P10 at 6.63 gal/bushel and P90 at 323 gal/bushel).

Table 6. State-Level Water Consumption Factors

State	Estimated Water Consumption (acre-ft)	2007 Corn Production (bushel)	WCF (gal/bushel)
Illinois	154,594	2,248,664,947	22.4
Indiana	131,564	959,947,232	44.7
Iowa	53,990	2,292,163,101	7.68
Minnesota	136,412	1,138,660,229	39.0
Missouri	214,599	439,417,160	159
Nebraska	3,612,422	1,426,459,812	825
Ohio	10,487	526,601,789	6.49
South Dakota	91,387	518,552,101	57.4
Wisconsin	66,178	437,174,706	49.3
Total	**4,471,630**	**9,987,641,077**	**146**

This record assumes that corn ethanol production consumes 2.7 and 3.92 gal of water per gallon of ethanol by dry- and wet-milling ethanol plants, respectively (Lampert et al. 2014).

3.4. Natural Gas Extraction and Processing

In the U.S., NG is largely produced from conventional and shale gas wells. In recent years, the share of shale gas production has been increased significantly, reaching 50% of U.S. NG production in 2015 (U.S. EIA 2016c). These NG extraction processes have different WCFs, which were summarized in Clark et al.

(2011). They estimated WCFs for conventional gas extraction at 0.071–0.155 gal/mmBtu, while shale gas extraction's WCFs were estimated at 1.095 to 8.034 gal/mmBtu, depending on shale gas plays (see Table 7). Based on these estimates, Lampert et al. (2014) estimated the average WCFs of conventional and shale gas extraction at 0.11 and 0.36 gal/mmBtu, respectively. This record developed triangular distributions for the WCFs of NG extraction by using the minimum and maximum WCFs reported in Clark et al. (2011).

Table 7. Water Consumption Associated with Shale Gas Recovery Operations in gal/mmBtu (Clark et al. 2011)

	Barnett	Marcellus	Fayetteville	Haynesville	Average
Min	1.50	2.09	2.33	1.10	1.75
Max	6.49	3.39	8.03	4.31	5.56

This record used the NG-processing WCF of 1.7 gal/mmBtu estimated by Gleick (1994). Since only one data point was available, no distribution was developed.

3.5. Coal Extraction and Processing

While decreasing substantially, coal still accounts for 34.3% of the total electricity generation mix in 2015 (U.S. EIA 2016c). Coal can be produced by either surface or underground mining. The water consumption in underground mining tends to be higher compared to surface mining, partly because water is often used to suppress dust for health and safety reasons (Gleick 1994).

Major U.S. states producing coal include Wyoming, West Virginia, Kentucky, Pennsylvania, and Texas. Gleick estimated WCFs of surface and underground mining at 1.7–1.9 and 1.9–6.7 gal/mmBtu, respectively. In addition, Grubert et al. (2012) reported that surface mining has a WCF of 16.1 gal/mmBtu. Based on these WCFs and coal production in 2011 reported by EIA (2012), Lampert et al. (2014) estimated the national average WCFs of surface and underground mining at 2.6 and 4.6 gal/mmBtu. This record developed a Weibull distribution for the WCF of surface mining using the minimum and maximum of the reported WCFs (1.7 and 16.1 gal/mmBtu) as the P0 and P90 of the distribution, respectively. Also, a triangular distribution was used for the WCF of underground mining.

3.6. Uranium Mining and Processing

Uranium fuel is produced through various processes: mining, milling, conversion, enrichment, fabrication, storage and disposal, and reprocessing of spent fuel. Meldrum et al. (2013) provided the median, minimum, and maximum of WCFs of these processes in gal/MWh of electricity from nuclear plants based on previous studies. Lampert et al. (2014) aggregated the WCFs in gal/gram of U-235 into three categories consistent with the GREET model structure: a mining/milling process, an enrichment process, and a conversion/storage/disposal process. This record uses the same aggregation to obtain the minimum and maximum WCFs to develop distribution functions as summarized in Table 3.

3.7. Woody Biomass Harvesting

Most cellulosic biomass resources are assumed to require no irrigation (U.S. Department of Energy 2016). Thus, this record also assumes no irrigation for woody biomass (hybrid poplar).

3.8. Electricity Generation

The 2015 U.S. average generation mix projected by EIA is used for this record as summarized in Table 8 (U.S. EIA 2016c). To obtain WCFs of electricity generation, GREET groups them into thermoelectric (including residual oil, NG, coal, nuclear and biomass), hydro, solar, wind, and geothermal power generation (Lee et al. 2016a).

Table 8. 2015 U.S. Average Generation Mix Projected by EIA (U.S. EIA 2016c)

Residual Oil	NG	Coal	Nuclear	Biomass	Hydroelectric	Geothermal	Wind	Solar	Others
0.6%	31.9%	34.3%	20.4%	0.2%	6.3%	0.4%	4.8%	0.6%	0.5%

3.8.1. Thermoelectric

Depending on the power cycle technology, thermoelectric power plants can be categorized into steam turbine, gas turbine, and combined cycle (a combination of steam and gas turbine). Since gas turbine cycles are powered directly by high enthalpy gas combustion in an open cycle, they do not consume any water. Lee et al. (2016b) investigated water consumption at a facility level using EIA-923 (U.S. EIA 2016b), which provides data on power generation, cooling, water withdrawal, and water consumption along with other general information on the power plants. They also cross-checked the information regarding the cooling tower provided in EIA-860 (U.S. EIA 2016a) with those in EIA-923. Since thermoelectric power plants (steam turbines or combined cycles) when using the same cooling technology but different fuels have similar WCFs, these plants are classified into six categories by cooling technology and prime mover rather than by fuel: (1) once-through cooling without a pond or a tower, (2) cooling with a pond (steam turbine), (3) cooling with a pond (combined cycle), (4) cooling with a tower (steam turbine), (5) cooling with a tower (combined cycle), and (6) dry cooling.

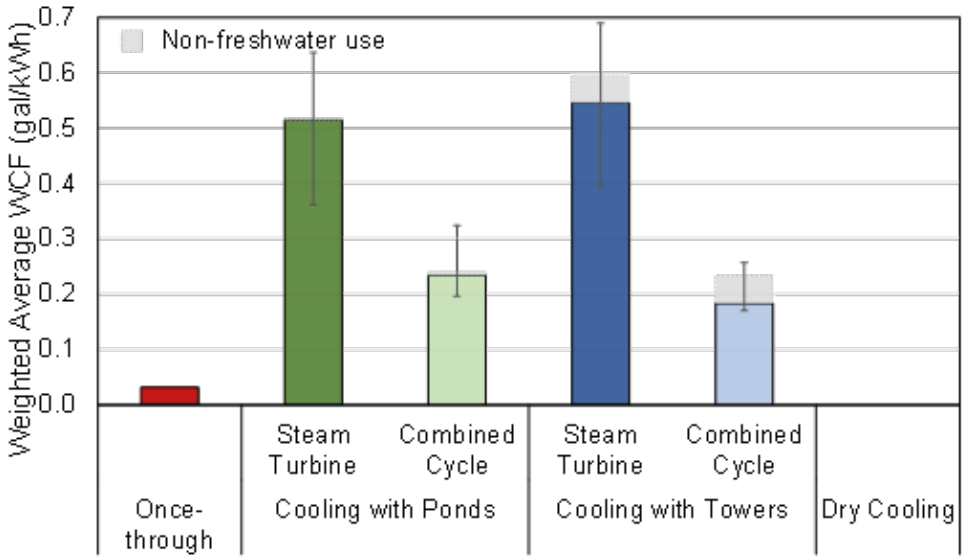

Figure 4. WCFs by Cooling Technology and Prime Mover

The resulting WCFs are presented in Figure 4. Note that some power plants use non-fresh water (saline, brackish water, or treated wastewater) for cooling, which was not included in the WCF calculations. The facility-level WCFs were aggregated by using power generation in 2015 to develop generation-weighted averages and distribution functions of steam turbine and combined-cycle WCFs, summarized in Table 3. The cumulative distributions of steam turbine and combined-cycle WCFs are presented in Figure 5.

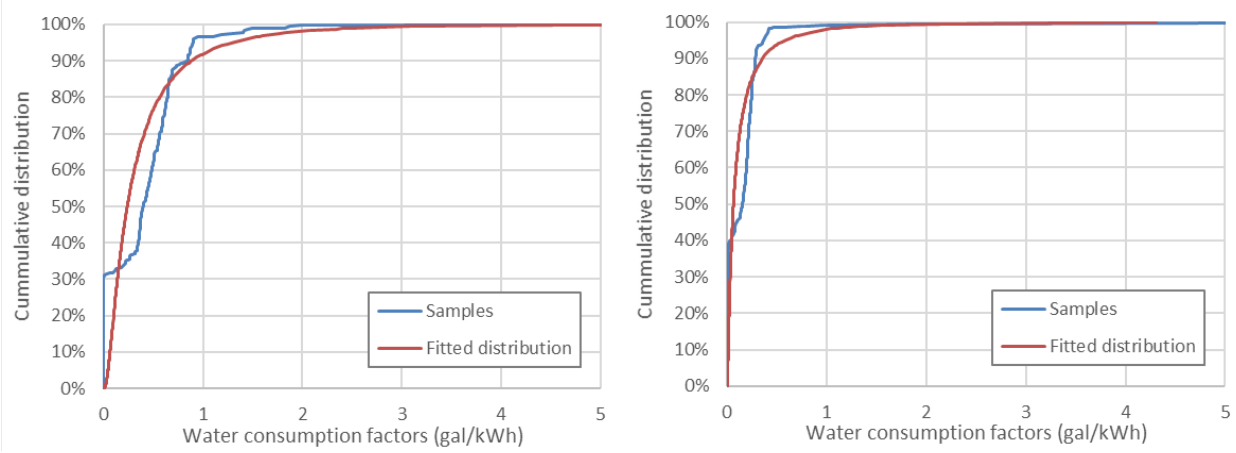

(a) Steam Turbine (b) Combined Cycle

Figure 5. Cumulative Distributions of Steam Turbine and Combined-Cycle WCFs

3.8.2. Hydro

Hydropower dams can be categorized into two groups: run-on-the-river (ROR) dams and dams with reservoirs. Both ROR dams and dams with reservoirs account for 22% and 78% of U.S. hydropower generation. Since an ROR dam uses natural river flow to generate electricity, it does not consume water. Lee et al. (2016b) calculated the WCFs of hydropower dams with reservoirs at a facility level by using regional annual water evaporation and evapotranspiration rates, reservoir surface area, and annual

power generation. Annual water evaporation rates were estimated from daily pan evaporation measured by the National Weather Service (NOAA 2016) and a ratio of 0.75 to correct for pan evaporation to lake evaporations (Lee et al. 2016b). Evapotranspiration rates were obtained by using a regression model developed by Sanford and Selnick (2013). Reservoir surface areas were collected from the National Inventory of Dams (NID) maintained by the Army Corps of Engineers (2016), which provides the location, reservoir surface area, and purposes of each dam in the United States. Finally, annual generation of hydropower electricity was obtained from the Emissions & Generation Resource Integrated Database (eGRID) by the U.S. Environmental Protection Agency (U.S. EPA 2012).

Of power generation from hydropower dams with reservoirs, 86% is generated from dams serving multiple purposes along with hydropower generation (such as irrigation, flood control, navigation, water supply, recreation, fire protection, fish and wildlife, debris control, and others). For these multipurpose dams, allocating the total water consumption by a multi-purpose reservoir to hydropower is an important factor for hydropower WCFs. Lee et al. (2016b) applied economic-benefit-based allocation factors developed by Hadjerioua et al. (2015). The allocation factors were developed for three levels of hydropower capacity and four levels of the number of purposes. On the basis of these allocation factors, allocated WCFs were estimated for individual hydropower dams and aggregated by annual generation to develop generation-weighted averages and distribution functions of WCFs of hydropower with reservoirs, as summarized in Table 3. The cumulative distributions of WCFs for hydropower with reservoirs are presented in Figure 6.

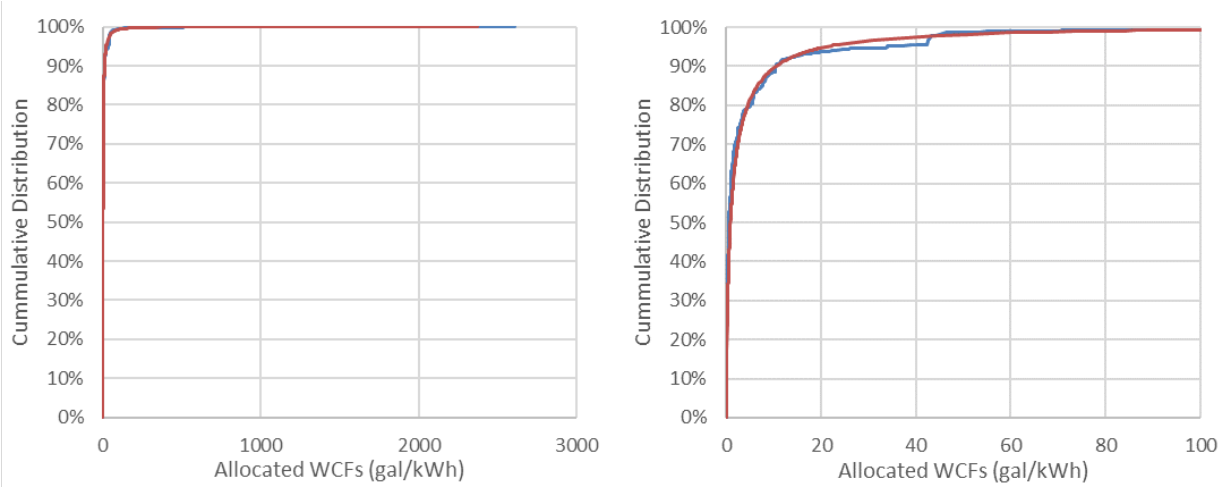

(a) x-axis: 0 – 3,000 gal/kWh (b) x-axis: 0 – 100 gal/kWh

Figure 6. Cumulative Distributions of WCFs for Hydropower with Reservoirs

3.8.3. Solar

Currently, PV or CSP plants account for 91% and 8% of U.S. total solar power generation, respectively (U.S. EIA 2016c). The water consumption associated with PV and CSP was summarized by Meldrum et al. (2013). The median, minimum, and maximum WCFs of PV and CSP in Meldrum et al. (2013) and the generation shares were used to determine the generation-weighted averages, as well as the P0 and P90 of the Weibull distribution for the WCF of solar power plants, as summarized in Table 3.

3.8.4. Wind

Meldrum et al. (2013) determined that 0–0.002 gal water per kWh of electricity is needed for cleaning, which this record used to develop the triangular distribution.

3.8.5. Geothermal

From the WCFs for various geothermal technologies summarized by Meldrum et al. (2013), Lampert et al. (2014) developed the WCFs for a flash plant, binary plant, and enhanced geothermal system (EGR). This record used the inventory by Meldrum et al. (2013) to develop triangular distributions for flash and binary plants and a Weibull distribution for EGR, as summarized in Table 3.

3.9. Hydrogen Production

3.9.1. Hydrogen from Natural Gas Steam Methane Reforming with and without CCS and Electrolysis

Elgowainy et al. (2015) estimated WCFs for hydrogen production via SMR and electrolysis in central production and distributed locations based on information acquired from industry, as summarized in Table 9. Among them, the amount of water discharged is eventually treated and discharged to the original water body. Thus, in Elgowainy et al. (2016a), the water discharge to water treatment processes was excluded by assuming negligible water consumption by the water treatment processes (Li et al. 2016). Based on the updated WCFs, triangular distributions were developed for a central SMR, while a Weibull distribution was used for the distributed SMR. No distribution was generated for electrolysis due to lack of data.

Table 9. WCFs for Hydrogen Production via SMR and Electrolysis in Central Production and Distributed Locations in gal/kg H_2

	SMR			Electrolysis	
Process	Central w/o CCS	Central w/CCS	Distributed	Central	Distributed
Water Treatment Process	0.7	0.75	3.3	3.9	3.9
Production Process	1.7 (1.5 – 1.8)	1.7 (1.5 – 1.8)	2.5 (2.4 – 3.0)	2.9	2.9
Cooling Loss	0.65	1.15	0	1.2	0
Total WCF					
Elgowainy et al. (2015)	3.1 (2.9 – 3.2)	3.6 (3.4 – 3.7)	5.8 (5.7 – 6.3)	8.0	6.8
Elgowainy et al. (2016a)	2.4 (2.2 – 2.5)	2.9 (2.7 – 3.0)	2.5 (2.4 – 3.0)	4.1	2.9

3.9.2. Hydrogen from Coal Gasification with CCS

Lampert et al. (2014) developed a WCF for coal gasification with CCS using the water consumption estimated by Rath (2010) for the state of the art for hydrogen production for several different cooling and process configurations. This record used the inventory by Rath (2010) to develop the triangular distribution provided in Table 3.

3.9.3. Hydrogen from Biomass Gasification

Elgowainy et al. (2016a) investigated the WCF of hydrogen production via biomass gasification using two data sources: Spath et al. (2005) and Choi et al. (2009). The resulting WCFs of H_2 from biomass gasification from these independent sources are 3.3 to 3.7 gal/kg H_2, excluding the water that goes into the water treatment processes. Using these data, this record developed the triangular distribution presented in Table 3.

4. References

Army Corps of Engineers. 2016. "CorpsMap: The National Inventory of Dams (NID)." http://nid.usace.army.mil/cm_apex/f?p=838:12.

Brandt, Adam R., Tim Yeskoo, Scottt McNally, Kourosh Vafi, Hao Cai, and Michael Q Wang. 2015. "Energy Intensity and Greenhouse Gas Emissions from Crude Oil Production in the Bakken Formation: Input Data and Analysis Methods." Argonne, IL: Argonne National Laboratory.

Brinkman, Norman, Michael Wang, Trudy Weber, and Thomas Darlington. 2005. "Well-To-Wheels Analysis of Advanced Fuel/Vehicle Systems—a North American Study of Energy Use, Greenhouse Gas Emissions, and Criteria Pollutant Emissions." Argonne, IL: Argonne National Laboratory.

Choi, DongWon, David C. Chipman, Scott C. Bents, and Robert C. Brown. 2009. "A Techno-Economic Analysis of Polyhydroxyalkanoate and Hydrogen Production from Syngas Fermentation of Gasified Biomass." *Applied Biochemistry and Biotechnology* 160 (4): 1032–46. doi:10.1007/s12010-009-8560-9.

Clark, Corrie E., Jeongwoo Han, Andrew Burnham, Jennifer B Dunn, and Michael Q. Wang. 2011. "Life-Cycle Analysis of Shale Gas and Natural Gas." ANL/ESD/11-11. Argonne, IL: Argonne National Laboratory.

Elgowainy, Amgad, Jeongwoo Han, Uisung Lee, Jeff Li, Jennifer Dunn, and Michael Wang. 2016a. "Life-Cycle Analysis of Water Consumption for Hydrogen Production." Argonne, IL: Argonne National Laboratory.

Elgowainy, Amgad, Jeongwoo Han, Jacob Ward, Fred Joseck, David Gohlke, Alicia Lindauer, Todd Ramsden, et al. 2016b. "Cradle-to-Grave Lifecycle Analysis of U.S. Light Duty Vehicle-Fuel Pathways: A Greenhouse Gas Emissions and Economic Assessment of Current (2015) and Future (2025-2030) Technologies." ANL/ESD-16/7. Argonne National Laboratory (ANL). http://www.osti.gov/scitech/biblio/1254857.

Elgowainy, Amgad, David J. Lampert, Hao Cai, Jeongwoo Han, Jennifer Dunn, and Michael Wang. 2015. "Life-Cycle Analysis of Water Use for Hydrogen Production Pathways." Argonne, IL: Argonne National Laboratory.

Ghandi, Abbas, Sonia Yeh, Adam R. Brandt, Kourosh Vafi, Hao Cai, Michael Q. Wang, Bridget R. Scanlon, and Robert C Reedy. 2015. "Energy Intensity and Greenhouse Gas Emissions from Crude Oil Production in the Eagle Ford Region: Input Data and Analysis Methods." Argonne, IL: Argonne National Laboratory.

Gleick, P. H. 1994. "Water and Energy." *Annual Review of Energy and the Environment* 19 (1): 267–99. doi:10.1146/annurev.eg.19.110194.001411.

Grubert, Emily A., Fred C. Beach, and Michael E. Webber. 2012. "Can Switching Fuels Save Water? A Life Cycle Quantification of Freshwater Consumption for Texas Coal- and Natural Gas-Fired Electricity." *Environmental Research Letters* 7 (4): 45801. doi:10.1088/1748-9326/7/4/045801.

Hadjerioua, B., A.M. Witt, K.M. Stewart, M. Bonnet Acosta, and M. Mobley. 2015. "The Economic Benefits of Multipurpose Reservoirs in the United States Federal Hydropower Fleet." ORNL/TM-2015/550. Oak Ridge, TN: Oak Ridge National Laboratory.

Henderson, Rob. 2016. “Water Consumption in US Petroleum Refineries.” Chicago, IL: Jacobs Consultancy.

Lampert, David, Hao Cai, Zhichao Wang, Jennifer Keisman, May Wu, Jeongwoo Han, Jennifer Dunn, et al. 2014. “Development of a Life Cycle Inventory of Water Consumption Associated with the Production of Transportation Fuels.” Argonne, IL: Argonne National Laboratory.

Lee, Uisung, Jeongwoo Han, Amgad Elgowainy, and Michael Wang. 2017. "Regional Water Consumption Factors for Hydro and Thermal Electricity Generation in the United States." *Applied Energy* In Press. https://doi.org/10.1016/j.apenergy.2017.05.025.

Lee, Uisung, Jeongwoo Han, and Hao Cai. 2016a. “Update of Electricity Generation Mix and Crude Oil Share.” Argonne, IL: Argonne National Laboratory.

Lee, Uisung, Jeongwoo Han, and Amgad Elgowainy. 2016b. “Water Consumption Factors for Electricity Generation in the United States.” Argonne, IL: Argonne National Laboratory.

Li, Qianfeng, Jeongwoo Han, and Amgad Elgowainy. 2016. “Industrial Wastewater Treatment in GREET®Model: Energy Intensity, Water Loss, Direct Greenhouse Gas Emissions, and Biogas Generation Potential.” Argonne, IL: Argonne National Laboratory.

Meldrum, J., S. Nettles-Anderson, G. Heath, and J. Macknick. 2013. “Life Cycle Water Use for Electricity Generation: A Review and Harmonization of Literature Estimates.” *Environmental Research Letters* 8 (1): 15031. doi:10.1088/1748-9326/8/1/015031.

NOAA. 2016. “National Weather Service.” http://www.weather.gov.

Rath, L. 2010. “Assessment of Hydrogen Production with CO_2 Capture, Volume 1: Baseline State-of-the-Art Plants.” DOE/NETL-2010/1434. Pittsburgh, PA: National Energy Technology Laboratory.

Sanford, Ward E., and David L. Selnick. 2013. “Estimation of Evapotranspiration Across the Conterminous United States Using a Regression with Climate and Land-Cover Data.” *Journal of the American Water Resources Association* 49 (1): 217–30. doi:10.1111/jawr.12010.

Solley, Wayne B., Robert R. Pierce, and Howard A. Perlman. 1998. “Estimated Use of Water in the United States in 1995.” USGS Numbered Series 1200. U.S. Department of the Interior, U.S. Geological Survey, Branch of Information Services. http://pubs.er.usgs.gov/publication/cir1200.

Spath, Pamela L, Andy Aden, T. Eggeman, Matthew Ringer, B. Wallace, and J. Jechura. 2005. “Biomass to Hydrogen Production Detailed Design and Economics Utilizing the Battelle Columbus Laboratory Indirectly-Heated Gasifier.” NREL/TP-510-37408. Golden, CO: National Renewable Energy Laboratory.

U.S. Department of Energy. 2016. “2016 Billion-Ton Report: Advancing Domestic Resources for a Thriving Bioeconomy, Volume 1: Economic Availability of Feedstocks.” ORNL/TM-2016/160. Oak Ridge, TN: Oak Ridge National Laboratory. https://energy.gov/sites/prod/files/2016/12/f34/2016_billion_ton_report_12.2.16_0.pdf.

U.S. EIA. 2008. “Annual Energy Review 2007.” http://www.eia.gov/emeu/aer/contents.html.

———. 2012. “Annual Energy Review 2011.” http://www.eia.gov/emeu/aer/contents.html.

———. 2016a. “Annual Electric Generator Data - EIA-860 Data File.” http://www.eia.gov/electricity/data/eia860.

———. 2016b. “Annual Electric Utility Data – EIA-906/920/923 Data File.” https://www.eia.gov/electricity/data/eia923.

———. 2016c. “Annual Energy Outlook 2016.” DOE/EIA-0383. Washington, D.C: U.S. Energy Information Administration.

U.S. EPA. 2012. “Emissions & Generation Resource Integrated Database (eGRID).” http://www.epa.gov/cleanenergy/energy-resources/egrid/index.html.

USDA. 2009. “NASS-National Agricultural Statistics Service.” http://www.nass.usda.gov/index.asp.

Wu, May, and Y. Chiu. 2011. “Consumptive Water Use in the Production of Ethanol and Petroleum Gasoline — 2011 Update.” ANL/ESD/09–1—Update. Argonne, IL: Argonne National Laboratory.